2-(4-(tetrahydro-2*H*-pyran-2-yloxy)-undecyl)-propane-1,3-diamminedichloroplatinum(II): A Novel Platinum Compound that Overcomes Cisplatin Resistance and Induces Apoptosis by Mechanisms Different from that of Cisplatin

Andrea Dietrich,*[,†] Thomas Mueller,[†] Reinhard Paschke,[‡] Bernd Kalinowski,[‡] Timo Behlendorf,[†] Franziska Reipsch,[†] Angelika Fruehauf,[†] Hans-Joachim Schmoll,[†] Charlotte Kloft,[§] and Wieland Voigt[†]

Department of Hematology/Oncology, Martin-Luther-University of Halle-Wittenberg, Halle/Saale, Germany, Department of Medical-Pharmaceutical Chemistry, Martin-Luther-University of Halle-Wittenberg, Halle/Saale, Germany, Department of Clinical Pharmacy, Institute of Pharmacy, Martin-Luther-University of Halle-Wittenberg, Halle/Saale, Germany

Received March 25, 2008

(4-(tetrahydro-2*H*-pyran-2-yloxy)R_1)R_2-diamminedichloroplatinum(II) complexes (**1**−**12**) consisting of CDDP linked to THP via aliphatic CH_2-spacers were tested in two TGCT cell lines. The most promising compound, 2-(4-(tetrahydro-2*H*-pyran-2-yloxy)-undecyl)-propane-1,3-diamminedichloroplatinum(II) (**12**), completely overcame CDDP resistance of 1411HP cells, correlating with increased and accelerated cellular platinum uptake and much faster initiation of apoptotic cell kill. At equitoxic IC_{90} concentrations, **12** induced accelerated DNA fragmentation and caspase −3 and PARP cleavages. In contrast, DNA platination rate was much lower as compared to CDDP and no upregulation of p53 as well as no initiation of cell cycle arrest were observed. Apoptosis induction by **12** could not be inhibited by pretreatment with caspase-specific inhibitor Z-VAD-Fmk and was accompanied by strong calcium release and generation of reactive oxygen species. To summarize, **12** overcomes CDDP resistance and induces programmed cell death with molecular features different from CDDP, suggesting that both drugs induce apoptosis through different initial pathways.

Introduction

Despite cisplatin (*cis*-diamminedichloroplatinum(II), CDDP)-based chemotherapy is curative in testicular germ cell tumors (TGCT)[a] and constitutes a component of standard treatment regimes for ovarian, cervical, bladder, head and neck, small-cell and non-small-cell lung cancers, the development of platinum drugs with improved antitumoral activity continues to be a productive field of research.[1] At this, the main focus concentrates on designing cytotoxic agents possessing either oral bioavailability, fewer side effects, or being able to circumvent intrinsic or acquired CDDP resistance, which is a major clinical problem.[2] TGC cancer is one of very few cancers having an inherent and unusual high sensitivity to CDDP. With the introduction of CDDP-containing chemotherapy, TGCT became a model of curable neoplasm.[3–5] Admittedly, patients refractory to CDDP-based chemotherapy continue to have a very poor prognosis.[6]

Although CDDP has a central role in TGCT treatment for the last three decades, its exact mechanism of action is not completely defined. It is supposed that CDDP enters cells by passive diffusion, although there is some evidence that uptake may occur by an active copper transporter Ctr1p.[7] Low intracellular chloride concentrations are essential for formation of activated electrophile mono- and diaquo-CDDP complexes, which can react with any nucleophile cellular targets. CDDP is a well-known DNA-damaging agent, and it is currently thought that DNA platination is an essential first step in its cytotoxic activity. So far, it is generally accepted that cytotoxic effects of CDDP are ascribed to its interaction with nucleophilic N7-sites of purine bases in DNA to form DNA−DNA intrastrand and interstrand cross-links and DNA−protein bonds. The most common adducts are 1,2-intrastrand cross-links between adjacent guanines. Nevertheless, only 1% of CDDP is linked to nuclear DNA.[8] Besides, mitochondrial DNA, RNA and other cellular components, including membrane phospholipids, cytoskeletal microfilaments, and thiol-containing proteins, are potent reactants for the platinum structure.[9,10]

Apoptosis, a type of programmed cell death controlling the development and homeostasis of multicellular organisms by elimination of aged, damaged, or mutated cells, has been shown to be the key cellular event responsible for exhibiting the anticancer activity of CDDP.[11] Two major death pathways initiating apoptosis were described. Intracellular stress signals as well as receptor-triggered stimuli may lead to activation of a central component of apoptotic machinery, the proteolytic system of caspases. Caspases were identified as a family of aspartic acid specific cysteine proteases, which are synthesized as precursors (procaspases) and are converted into active enzymes by apoptotic stimuli. The "intrinsic" pathway involves initially the release of cytochrome c from mitochondria into cytosol and formation of the so-called complex "apoptosome" in the presence of apoptotic protease activating factor 1 (APAF-1), caspase -9 and dATP resulting in caspase -9 activation. The "extrinsic" pathway is induced by activation of death receptors like Fas or tumor necrosis factor receptor 1 (TNFR-1) in response to ligand binding and subsequent autocatalytic activation of caspase -8. Initiation of both processes finally result in cleavage and activation of effector caspases -3, -6, and -7 and cellular protein degradations, e.g., poly(ADP-ribose) polymerase

* To whom correspondence should be addressed. Phone: +49-345 5577278. Fax: +49-345 5577279. E-mail: andrea.dietrich@medizin.uni-halle.de. Address: Department of Hematology/Oncology, Klinikum Kröllwitz, Ernst-Grube-Strasse 40, 06120 Halle/Saale, Germany.

† Department of Hematology/Oncology, Martin-Luther-University of Halle-Wittenberg.

‡ Department of Medical-Pharmaceutical Chemistry, Martin-Luther-University of Halle-Wittenburg.

§ Department of Clinical Pharmacy, Institute of Pharmacy, Martin-Luther-University of Halle-Wittenburg.

[a] Abbreviations: CDDP, cisplatin; TGCT, testicular germ cell tumor; THP, tetrahydropyrane.

10.1021/jm800334z CCC: $40.75
Published on Web 08/13/2008

(PARP), and consequently in an irreversible commitment to apoptotic cell death.[12–14]

An important mediator of CDDP-provoked apoptosis is the tumor suppressor protein p53, which possess a dual role in stress response. P53 has been reported to be capable to arrest cells at G_1/S- and possibly G_2/M-checkpoints, mediating their DNA repair or initiate apoptosis if damage is irreparable. Additionally, p53 induces the pro-apoptotic Bcl-2 family member Bax without nuclear DNA damage.[15,16] Inactivation of p53 may contribute to hypersensitivity as well as chemotherapeutical resistance toward CDDP depending on kind of tumor cell type. Thus, p53 function is not always required for apoptosis.[17]

Considerable efforts have been invested in defining cellular and molecular principles responsible for CDDP resistance. Studies have shown that mechanisms underlying tumorresistance are multifactorial. These involve impaired drug uptake or enhanced drug efflux, increased cellular detoxification due to increased thiol-containing species such as glutathione and metallothioneins, strengthened tolerance of DNA adducts, and increased repair of platinum-mediated DNA damage.[15,18] Occurrence of resistance contributes to a decreased susceptibility for induction of apoptosis and to loss of the cytoreductive effects of CDDP. Overcoming clinical resistance has proven particularly difficult. So far, therapeutically used platinum analogues like carboplatin, nedaplatin, and lobaplatin yield cross-resistance with CDDP and many derivatives had abandoned already in clinical trials. Thus, strategies of platinum drug research orient toward designing complexes capable of circumventing CDDP resistance by innovative "nonclassic" platinum structures with altered pattern of DNA binding, e.g., multinuclear platinum, platinum(IV), or active *trans*-platinum compounds with planar, iminoether, or ammine ligands.[19,20]

The multinuclear platinum derivative BBR3464 ([{*trans*-$PtCl(NH_3)_2$}$_2${μ-*trans*-$Pt(NH_3)_2(NH_2(CH_2)_6NH_2)_2$}]$(NO_3)_4$) for instance represents a trinuclear bifunctional compound in which two monofunctional *trans*-platinum units are linked with a tetraammine. BBR3464 is marked by the ability of bypassing the p53-mediated apoptotic pathway and the capability of breaking CDDP resistance, implemented by higher intracellular platinum accumulation and accelerated formation of DNA adducts as compared to CDDP.[21,22] The oral applicable ZD0473 (AMD473, *cis*-amminedichloro(2-methylpyridine)platinum(II)) circumvents CDDP resistance using a spatial shielding of platinum by a methyl-substituted pyridine ring. This sterically delimitation induces a reduced susceptibility regarding its cellular detoxification by glutathione, metallothioneins, and other cellular thiols.[19] A further group of new-generation agents are the family of Bamets (**b**ile **a**cid, **met**al; including Bamet-UD2 (*cis*-diamminechlorocholylglycinateplatinum(II)). Coupling of platinum structures to bile acids as biological active shuttles improves their targeting toward liver tumors and enhances their availability in tumors. Consequently, a more selective chemotherapy as well as an efficiently response of tumor tissues by targeted transport can be achieved.[23–25]

Recently, our group reported about a new CDDP conjugate ChAPt-11 consisting of a **ch**olic **a**cid linked to cis**pl**a**t**in by a **C_{11}**-alkyl spacer. It was designed originally with the aim of selective enrichment in gut and liver by reabsorption of cholic acid in enterohepatic circulation. However, as the more interesting finding it revealed the ability to circumvent CDDP resistance in a primary resistant TGCT cell line.[26,27] The present paper summarizes the cytotoxic evaluation of (4-(tetrahydro-2*H*-pyran-2-yloxy)-R_1)R_2-diamminedichloroplatinum(II) compounds (**1**−**12**),[27–29] in which 2-(4-(tetrahydro-2*H*-pyran-2-yloxy)-undecyl)-propane-1,3-diamminedichloroplatinum(II) (**12**) was identified as the most promising substance, showing a remarkable cytotoxic response in a panel of TGCT cell lines. Following the cellular and molecular principles underlying **12**-initiated cell death as compared to CDDP were described using the CDDP-sensitive TGCT cell line H12.1 and the CDDP-resistant TGCT cell line 1411HP as tumor models.

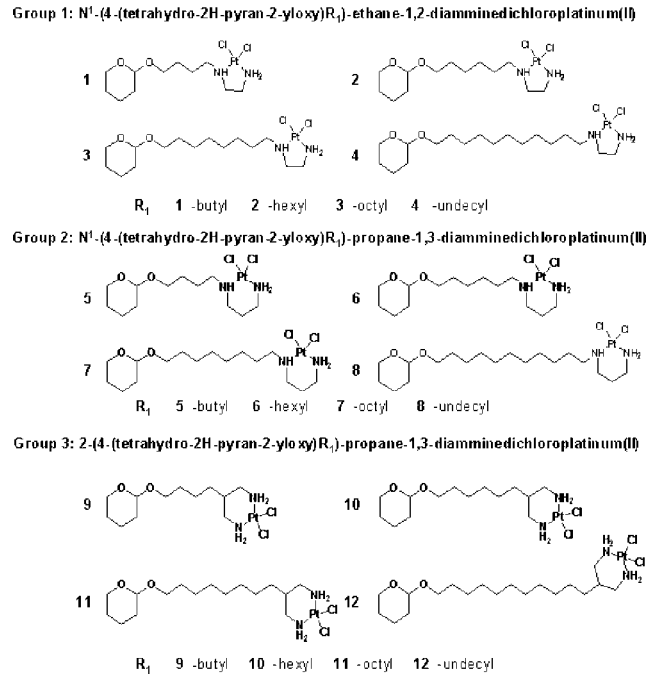

Figure 1. Structures of THP platinum compounds **1**−**12**. Group 1 N^1-(4-(tetrahydro-2*H*-pyran-2-yloxy)R_1)-ethane-1,2-diamminedichloroplatinum(II), group 2 N^1-(4-(tetrahydro-2*H*-pyran-2-yloxy)R_1)-propane-1,3-diamminedichloroplatinum(II), group 3 2-(4-(tetrahydro-2*H*-pyran-2-yloxy)R_1)-propane-1,3-diamminedichloroplatinum(II); R_1: -butyl/ -hexyl/ -octyl/ -undecyl.

Results

Cytotoxic Activity of THP Platinum Compounds 1−12 and CDDP in CDDP-Sensitive and CDDP-Resistant TGCT Cell Lines. Dependent on the way of linking the THP-alkyl spacer to CDDP, the designed (4-(tetrahydro-2*H*-pyran-2-yloxy)R_1)R_2-diamminedichloroplatinum(II) compounds **1**−**12** could be classified into three groups. Within each group, the substances differ with respect to the alkyl spacer length (Figure 1). Rating their cytotoxic potential compared to CDDP was implemented by SRB-assay using the CDDP-sensitive H12.1 and the CDDP-resistant 1411HP (Table 1). Comparison of the groups revealed a trend of enhanced efficacy with increased alkyl spacer length. Accordingly, the highest activity was found for the C_{11}-spacer derivatives **4**, **8**, and **12**. In the C_{11}-spacer derivatives group, **12** (combining CDDP and spacer by symmetrically carbon-linked propylene diammine) exerted the strongest cytotoxic potential followed by **8** (defined by nitrogen-linked propylene diammine) and **4** (defined by nitrogen-linked ethylene diammine). Moreover, **12** was able to completely overcome the CDDP-resistance of 1411HP. Therefore, we selected **12** to further investigate its cytotoxic potency in a panel of TGCT cell lines with different CDDP sensitivity (Table 2). Comparison of **12** and CDDP on the level of IC_{50} and IC_{90} after 2 h exposure revealed a higher activity of **12** in all tested cell lines and a lack of cross resistance to CDDP. In contrast, after 96 h continuous drug exposure, only primary cisplatin resistant cell lines 1777NRpmet and 1411HP were more sensitive to **12** as compared to CDDP.

Table 1. Cytotoxic Activities of CDDP and THP Platinum Compounds **1**−**12** in Human TGCT Cell Lines H12.1 (CDDP-Sensitive) and 1411HP (CDDP-Resistant)[a]

platinum compound	IC_{50} [μM] 96 h cell line H12.1	IC_{50} [μM] 96 h cell line 1411HP	resistance factor	*p*-value
CDDP	0.7	2.8	3.8	>0.05
1	11.0	28.5	2.6	<0.001
2	13.0	29.0	2.2	<0.01
3	20.0	12.3	0.6	>0.05
4	**10.3**	**4.7**	0.5	>0.05
5	12.7	11.7	0.9	>0.05
6	11.0	8.7	0.8	>0.05
7	6.0	5.3	0.9	>0.05
8	**5.7**	**4.3**	0.8	>0.05
9	9.3	28.3	3.0	<0.001
10	13.3	13.0	1.0	>0.05
11	5.3	5.8	1.1	>0.05
12	**1.8**	**1.7**	0.9	>0.05

[a] IC_{50} values (μM) of CDDP and **1**−**12** after 96 h treatment using H12.1 and 1411HP. The concentrations of CDDP or platinum compound, which inhibited cell growth by 50% (IC_{50}), were determined from semilogarithmic concentration−response plots. The resistance factor (IC_{50} 1411HP/IC_{50} H12.1) indicates the enhanced drug demand to achieve an equitoxic response in 1411HP. Data represent means of three individual experiments.

Cytotoxicity studies of THP-C_{11}-alkyl spacer without platinum substitution revealed no relevant antitumoral activity as compared to the parental drug in both tumor models. Furthermore, 96 h treatment of H12.1 and 1411HP with THP-C_{11}-alkyl spacer mixed with CDDP resulted in an efficacy similar to exposure with CDDP alone (data not shown).

On the basis of data presented, the most promising drug **12** showed the highest cytotoxic activity and was able to completely overcome resistance of 1411HP and 1777NRpmet. In subsequent studies, investigating the underlying mechanisms of CDDP and **12**-induced cytotoxicity equitoxic IC_{90} concentrations were used as follows: H12.1 CDDP 30 μM/3 μM (2 h/24 h), 1411HP CDDP 100 μM/10 μM (2 h/24 h), and for both **12** 2.5 μM/2.5 μM (2 h/24 h). Note that IC_{90} concentrations of a 24 h treatment regime of CDDP and **12** were identical with IC_{90} concentrations of a 96 h treatment schedule (data not shown).

Platinum Drug Accumulation Studies of 9, 10, 12, and CDDP. To investigate if differences in platinum accumulation contribute to the diverse cellular response to **12** and CDDP, intracellular platinum uptake of equitoxic IC_{90} concentrations was determined (Figure 2A). Treatment of 1411HP with CDDP for 2 h resulted in 3.7-fold higher platinum uptake as compared to H12.1. Exposure to **12** for 2 h resulted in a platinum accumulation, which was significant 8.7-fold higher in H12.1 and 4.4-fold higher in 1411HP as compared to CDDP. Furthermore, **12** was significantly 1.9-fold more enriched in 1411HP than in H12.1.

To analyze the influence of the alkyl spacer length on platinum uptake, H12.1 and 1411HP were treated with equimolar concentrations (30 μM) of CDDP, **9**, **10**, and **12** for 2 h (Figure 2B). There was an obvious positive correlation between platinum uptake and spacer length. Again, the highest amount of platinum was measured after treatment with **12** and uptake in 1411HP was slightly higher as compared to H12.1. Taken together, there was a clear relationship between drug structure and accumulation with the highest drug uptake found for **12**. Notably, total platinum uptake was higher in resistant 1411HP cells.

Characterization of Genomic DNA Platination Capacity of 12 and CDDP. Because DNA is the supposed primary cellular target of platinum drugs, DNA platination by **12** and CDDP was examined (Figure 2C). Treatment with equimolar concentrations (30 μM) of both drugs for 6 h resulted in significant 18.7-fold higher accumulation of **12** in H12.1 and significant 31.2-fold higher uptake of **12** in 1411HP as compared to CDDP. Again, **12** content was significantly 1.9-fold higher in 1411HP as compared to H12.1. However, the rate of DNA platination was significantly 9.6-fold (H12.1) respectively 3.8-fold (1411HP) higher in CDDP-exposed than **12**-exposed cells. In relation to cellular drug uptake, 13.7% (H12.1) respectively 11.1% (1411HP) of accumulated CDDP bound to DNA, whereas only 0.1% of total intracellular **12** could be recovered on DNA of H12.1 and 1411HP cells. Further support for this notion comes from cell free DNA-binding studies using naked plasmid DNA. After treatment with equimolar concentrations of CDDP and **12**, an obvious mobility shift in the DNA agarose gel for CDDP was observed, whereas no effect occurred in the **12**-treated group (data not shown). Thus, despite its much higher uptake, **12** appears to have a very low DNA-binding capacity.

Comparison of 12- and CDDP-Induced Cell Death: Analysis of DNA Laddering. On the basis of the promising cytotoxic potential and the low DNA platination despite increased cellular uptake, molecular mechanisms underlying **12**-induced cell death should be further examined. To test whether **12**-initiated cell death is mediated by apoptosis, floating cells of H12.1 and 1411HP after treatment with **12** or CDDP were analyzed with DNA gel electrophoresis. In both cell models, occurrence of typical DNA laddering was observed after 24 h treatment with appropriate IC_{90} concentrations (data not shown). Furthermore, programmed cell death was confirmed by trypan-blue exclusion test in which floating cells still showed ability to exclude the blue dye (data not shown). Thus, **12** like CDDP kills cells by induction of apoptosis.

Comparison of Cell Cycle Perturbations and Apoptotic Mechanisms Induced by 12 and CDDP.

Cell Cycle Perturbations. For analysis of cell cycle perturbations induced by CDDP or **12**, exponentially growing H12.1 and 1411HP cells were treated with equitoxic IC_{90} concentrations of CDDP and **12** (Figure 3 and Table 3). Compared to control, CDDP (IC_{90} 24 h) caused an S-phase arrest in H12.1 and a slight S-phase accumulation in 1411HP cells after 24 h. After an additional 24 h, about 21% of H12.1 and already nearly half of all 1411HP underwent cell death (as indicated by $SubG_1$-peak). In contrast to CDDP, treatment with **12** (IC_{90} 2 h/24 h) did not induce significant cell cycle arrest in any cell cycle phase but rather directly provoked an increase of $SubG_1$-peak with concomitant decline of all other cell cycle phases in H12.1 and 1411HP cells. Of particular note, no significant increase of the S-phase population could be observed over time. Finally, after 72 h exposure 57.3% (H12.1) respectively 91.4% (1411HP) cells were located to $SubG_1$-peak as compared with 38.4% (H12.1) respectively 48.8% (1411HP) CDDP-treated cells. In general, **12** appears to induce apoptosis significantly faster than CDDP as judged by the increase of $SubG_1$-peak over time.

p53 Accumulation. To clarify the apoptotic mechanisms triggered by **12** or CDDP in H12.1 and 1411HP, regulation of p53 was assessed by Western blot analyses (Figure 4A). The results showed a marked accumulation of p53 in H12.1 and 1411HP exposed to CDDP after 8 h (IC_{90} 2 h) and 24 h (IC_{90} 2 h and 24 h). On the other hand, compared with CDDP, nearly no modulation of p53 was found in both cell lines after 8 h and 24 h exposure to **12** (IC_{90} 2 h and 24 h).

Table 2. Activity Pattern of **12** and CDDP in a Panel of Human TGCT Cell Lines[a]

	IC_{50} [μM] 2 h				IC_{50} [μM] 96 h			
cell line	CDDP	**12**	increase in efficiency by **12**	*p*-value	CDDP	**12**	increase in efficiency by **12**	*p*-value
H12.1	7.9	1.8	4.5	<0.001	0.7	1.8	0.4	>0.05
H12.5	3.4	1.8	1.9	>0.05	0.6	1.8	0.3	>0.05
833K	2.8	1.4	1.9	>0.05	0.2	1.5	0.1	>0.05
2102EP	3.8	1.8	2.1	<0.05	0.5	1.7	0.3	>0.05
577MF	5.0	1.2	4.1	>0.05	0.7	0.9	0.8	>0.05
1777NRpmet	**12.4**	**1.7**	7.4	<0.001	**1.3**	**1.5**	0.8	>0.05
1411HP	**27.7**	**1.6**	17.3	<0.001	**2.8**	**1.7**	1.7	>0.05

	IC_{90} [μM] 2 h				IC_{90} [μM] 96 h			
cell line	CDDP	**12**	increase in efficiency by **12**	*p*-value	CDDP	**12**	increase in efficiency by **12**	*p*-value
H12.1	26.0	2.5	10.3	<0.001	2.8	2.5	1.1	>0.05
H12.5	16.3	2.5	6.5	<0.001	1.6	2.5	0.6	>0.05
833K	16.7	2.4	6.9	<0.001	1.4	2.4	0.6	>0.05
2102EP	14.5	2.8	5.2	<0.001	1.1	2.7	0.4	>0.05
577MF	25.3	2.3	11.2	<0.001	2.5	1.8	1.4	>0.05
1777NRpmet	>**100**	**2.5**	>40	<0.001	**8.2**	**2.5**	3.3	>0.05
1411HP	**80.0**	**2.5**	32.4	<0.001	**7.2**	**2.5**	2.9	>0.05

[a] IC_{50} and IC_{90} values (μM) of CDDP and **12** after 2 h and 96 h treatment of TGCT cell lines with different CDDP sensitivity. In the case of the 2 h treatment schedule, cells were washed after 2 h and supplemented with drug-free media for 94 h. The concentrations of CDDP or **12**, which inhibited cell growth by 50% (IC_{50}) or 90% (IC_{90}), were determined from semilogarithmic concentration−response plots. Data represent means of three individual experiments.

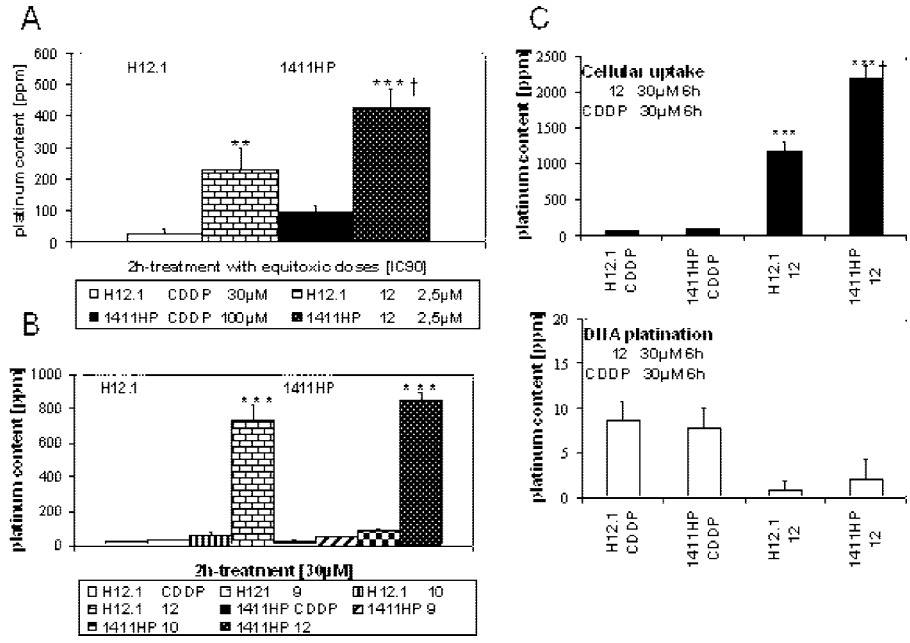

Figure 2. Platinum uptake studies of CDDP and THP platinum compounds in H12.1 and 1411HP cells quantified by AAS. Values represent means ± SD of three independent experiments. (A) Cellular platinum uptake of equitoxic IC_{90} concentrations of CDDP and **12** after 2 h treatment expressed as platinum content [ppm] in lyophilized cells (original weight 20−300 μg; **: significant to CDDP treated H12.1, $p < 0.01$; ***: significant to CDDP treated 1411HP, $p < 0.001$; †: significant to **12** treated H12.1, $p < 0.01$). (B) Cellular platinum uptakes of equimolar concentrations (30 μM) of CDDP, **9**, **10**, and **12** after 2 h treatment expressed as platinum content [ppm] in lyophilized cells (original weight 20−300 μg; ***: significant to CDDP, **9**, and **10**, $p < 0.001$). (C) Cellular platinum uptakes and DNA platination of equimolar concentrations (30 μM) of CDDP and **12** after 6 h treatment expressed as platinum content [ppm] in lyophilized cells or lyophilized genomic DNA (original weight 20−300 μg; ***: significant to CDDP, †: significant to **12** treated H12.1, $p < 0,001$).

Caspase -3 and PARP Cleavages. The results of Western blot analyses of caspase -3 and PARP cleavages in H12.1 and 1411HP cells are shown in Figure 4A. In both cell lines, procaspase -3 was activated differently after **12** and CDDP treatment, evidenced by occurrence of cleavage fragments p-17/p-20. Fragments of caspase -3 appeared yet 8 h after exposure to **12** (IC_{90} 2 h/24 h) in H12.1 and 1411HP cells. In contrast, treatment with CDDP (IC_{90} 2 h) for 8 h resulted in an only slight increase of cleavage fragments of caspase -3. After 24 h CDDP exposure, fragments clearly occurred in both cell lines (IC_{90} 2 h and 24 h). Besides, activation of caspase -3 caused by CDDP and **12** was paralleled with cleavage of PARP in H12.1 and 1411HP cells, as demonstrated by presence of the p-85 proteolytic fragment.

To examine participation of cytochrome c in the apoptotic process, H12.1 and 1411HP were exposed to both drugs and cytosolic extracts were prepared 8 h post drug treatment. Both CDDP (IC_{90} 24 h) and **12** (IC_{90} 2 h/24 h) caused a release of cytochrome c at 8 h time point. However, although treatment was conducted with equitoxic drug concentrations, cytochrome c release was more pronounced in **12**-treated cells (data not shown).

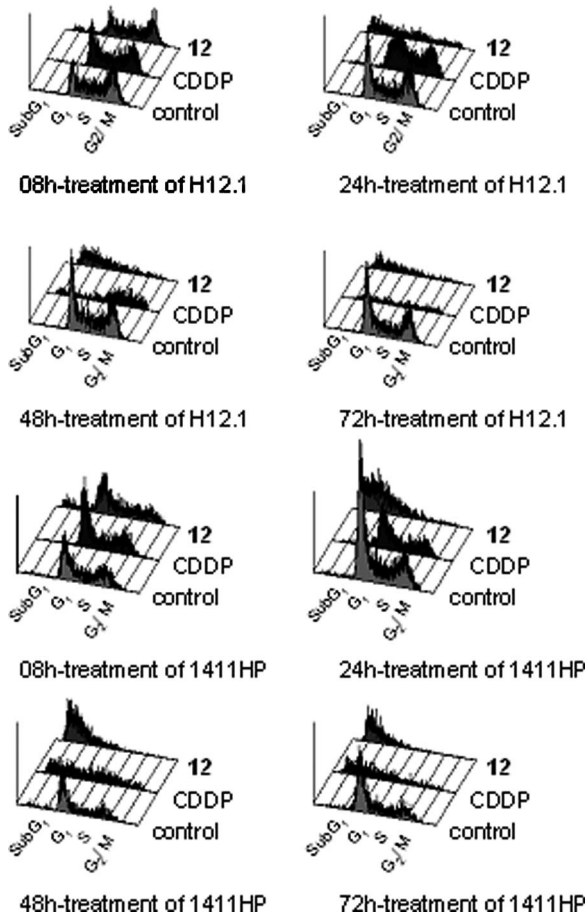

Figure 3. Cell cycle perturbations in H12.1 and 1411HP following treatment with CDDP (IC_{90} 24 h) and **12** (IC_{90} 2 h/24 h) analyzed by FACS. Experiments were performed three times, and representative DNA histograms are shown.

Caspase -3 Kinetic Studies. To discriminate the speed of apoptosis initiation by **12** and CDDP, caspase -3 activation was examined by substrate cleavage assay as a time kinetic (Figure 4B). In H12.1 and 1411HP cells, exposure to CDDP (IC_{90} 24 h) induced a delayed increase of caspase -3 activity, whereas after exposure to CDDP (IC_{90} 2 h), an accelerated and stronger activation could be observed. However, **12** (IC_{90} 2 h/24 h) caused an obviously even more accelerated caspase -3 activation. Caspase -3 activation by **12** peaked already after 8 h (H12.1) respectively 11 h (1411HP) of treatment, whereas the earliest peak for CDDP could be observed at about 18 h time point depending on CDDP concentrations in both cell lines. Concomitant to increase of caspase -3 activity, a growing population of floating cells became visible over time. Assessment of other apoptosis-relevant caspases, like caspase -2, -8, and -9 resulted in a similar manner of activation (data not shown).

Treatment with Caspase-Specific Inhibitor Z-VAD-Fmk. To delineate the importance of caspases in **12**- and CDDP-induced apoptosis, the broad spectrum caspase inhibitor Z-VAD-Fmk (Axxora) was used (Figure 4C). Pretreatment with inhibitor blocked cleavage of caspase -3 and suppressed execution of apoptosis in CDDP exposed H12.1 and 1411HP cells after 24 h and 48 h (IC_{90} 24 h). In contrast, **12** treatment (IC_{90} 2 h/24 h) still induced strong occurrence of floating H12.1 and 1411HP cells after 24 h and 48 h despite lacking caspase -3 cleavage. Apoptotic cell death in these floating cells was proven by DNA laddering (Figure 4D) and trypan-blue exclusion test (data not shown).

Table 3. Impact of Treatment with **12** or CDDP on Cell Cycle Progression in Human TGCT Cell Lines H12.1 and 1411HP[a]

	SubG$_1$	G$_1$	S	G$_2$/M
		H12.1		
control 08 h	2.8 ± 1.9	18.4 ± 2.6	43.8 ± 2.0	33.7 ± 4.3
control 24 h	2.9 ± 1.9	29.7 ± 3.0	**38.2 ± 3.2**	27.5 ± 2.1
control 48 h	2.3 ± 0.6	32.3 ± 4.3	36.1 ± 3.3	27.6 ± 1.2
control 72 h	3.5 ± 0.8	38.0 ± 3.8	33.8 ± 2.1	23.4 ± 2.0
CDDP 3 μM 08 h	1.3 ± 0.4	24.3 ± 1.3	46.1 ± 2.2	26.6 ± 2.1
CDDP 3 μM 24 h	3.1 ± 1.8	14.0 ± 5.0	**56.4 ± 3.2**	26.8 ± 6.0
CDDP 3 μM 48 h	20.7 ± 10.4	5.1 ± 1.1	38.0 ± 11.2	30.6 ± 7.0
CDDP 3 μM 72 h	38.4 ± 8.1	10.2 ± 2.1	29.7 ± 5.4	19.6 ± 3.8
12 2.5 μM 08 h	9.1 ± 1.6	15.1 ± 1.0	39.9 ± 3.0	33.1 ± 0.6
12 2.5 μM 24 h	**53.4 ± 3.7**	10.2 ± 2.4	**23.6 ± 3.8**	11.0 ± 3.9
12 2.5 μM 48 h	**67.5 ± 9.0**	10.3 ± 2.3	16.1 ± 4.2	4.4 ± 1.8
12 2.5 μM 72 h	**57.3 ± 12.3**	12.5 ± 1.8	22.3 ± 7.0	6.1 ± 2.9
		1411HP		
control 08 h	3.4 ± 0.8	34.1 ± 6.7	37.9 ± 4.3	22.7 ± 2.9
control 24 h	4.6 ± 1.2	38.6 ± 6.1	**33.3 ± 2.9**	20.9 ± 3.6
control 48 h	10.2 ± 4.2	37.6 ± 7.3	33.2 ± 4.2	17.0 ± 4.4
control 72 h	10.8 ± 2.5	41.4 ± 4.5	31.0 ± 1.6	14.6 ± 1.5
CDDP 10 μM 08 h	2.9 ± 0.9	42.6 ± 5.2	37.6 ± 5.1	15.4 ± 2.1
CDDP 10 μM 24 h	11.6 ± 3.1	26.1 ± 5.2	**43.4 ± 3.0**	17.1 ± 1.8
CDDP 10 μM 48 h	45.3 ± 5.4	12.0 ± 2.5	31.2 ± 3.8	9.1 ± 3.0
CDDP 10 μM 72 h	48.8 ± 8.9	11.4 ± 0.8	26.8 ± 4.8	10.3 ± 4.2
12 2.5 μM 08 h	20.3 ± 7.9	28.3 ± 1.0	32.5 ± 5.4	16.2 ± 2.4
12 2.5 μM 24 h	**73.3 ± 5.0**	11.4 ± 1.5	**12.8 ± 3.3**	1.6 ± 0.5
12 2.5 μM 48 h	**89.3 ± 7.8**	5.0 ± 2.9	4.5 ± 3.8	0.4 ± 0.4
12 2.5 μM 72 h	**91.4 ± 3.9**	4.6 ± 1.7	3.2 ± 1.8	0.4 ± 0.2

[a] Percentages of H12.1 and 1411HP cells distributed to cell cycle phases after treatment with CDDP or **12**. Values represent means ± SD of three individual experiments.

Calcium Homeostasis and Reactive Oxygen Species (ROS) Generation. The data from the previous experiments suggested that **12** induces apoptosis by an alternative mechanism, which could bypass the caspase-dependent pathway after blockage with a broad spectrum caspase inhibitor. To identify such mechanisms, further experiments were conducted including studies of the regulation of intracellular calcium release and formation of ROS. Results of a narrow time kinetic on cellular calcium homeostasis in H12.1 and 1411HP treated with IC_{90} concentrations (2 h) of **12** or CDDP are shown in Figure 5A. In both tumor models, CDDP (IC_{90} 2 h) caused an only slight release of free calcium into cytosol. In contrast, treatment with **12** (IC_{90} 2 h/24 h) resulted in a significant elevation of cytosolic free calcium in H12.1 as well as in 1411HP cells over time. At the 2 h time point, a significant 1.4-fold (H12.1) respectively 1.3-fold (1411HP) higher cytosolic calcium content as compared to CDDP was detected.

To analyze if **12**- or CDDP-induced apoptosis involves the generation of ROS lucigenin assay was performed detecting the formation of superoxide anion radicals ($O_2^{-\bullet}$) (Figure 5B). Treatment of 1411HP cells with **12** for 2 h (IC_{90} 2 h/24 h) led to a significant induction of radical generation, whereas no significant effect could be observed for CDDP (IC_{90} 2 h). In contrast, in H12.1 cells, neither **12** nor CDDP provoked a significant formation of $O_2^{-\bullet}$.

To summarize, in contrast to CDDP, **12** caused nearly no p53 accumulation as well as no cell cycle arrest. Besides, similar but accelerated cleavages of caspase -3 and PARP were induced. Treatment with caspase-specific inhibitor Z-VAD-Fmk did not inhibit apoptosis induction after treatment with **12**, but blocked execution of apoptosis after treatment with CDDP. Furthermore, in contrast to CDDP, **12** provoked a strong cytosolic calcium

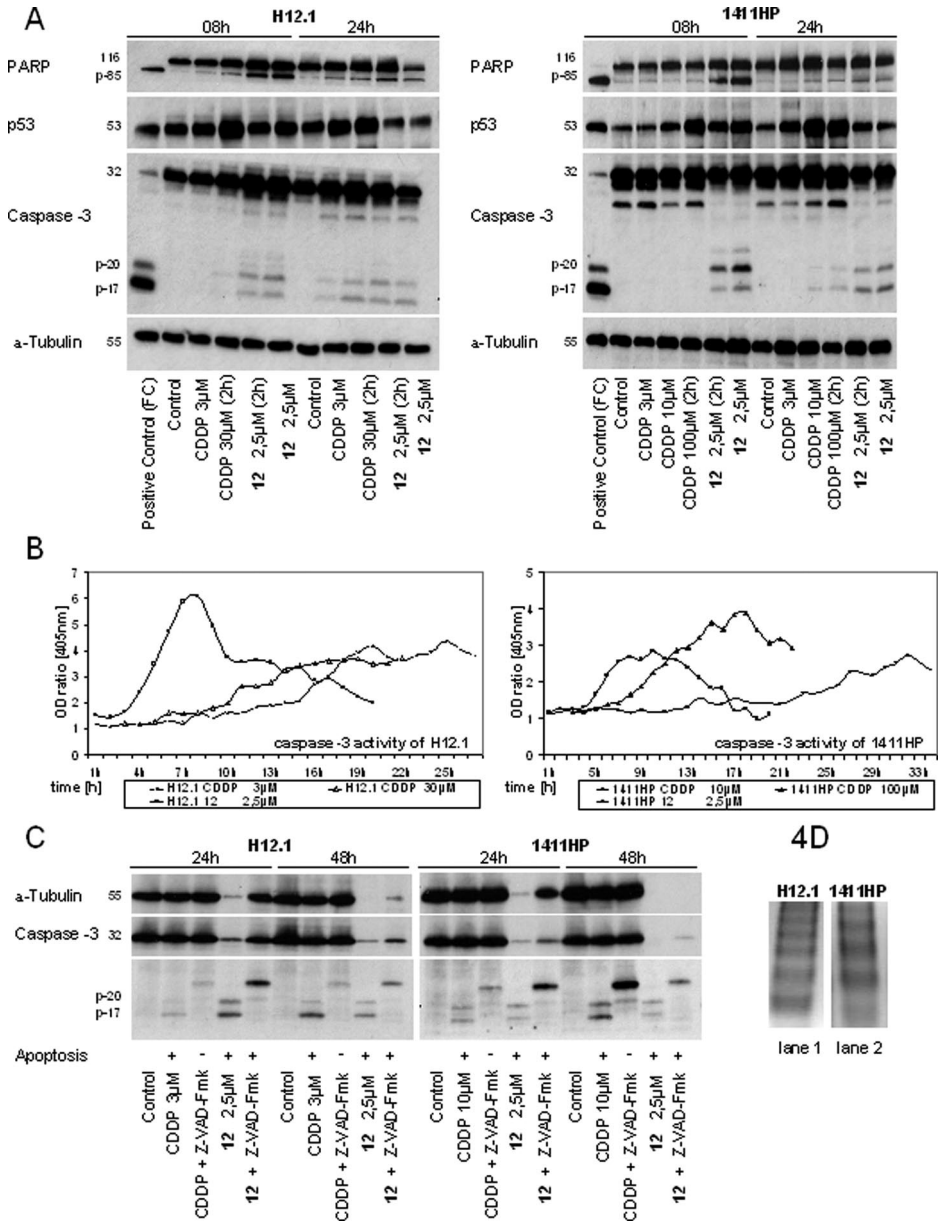

Figure 4. Analysis of apoptotic pathways triggered by CDDP and **12** in H12.1 and 1411HP cells. (A) and Western blot analyses of p53 expression and caspase -3 and PARP cleavages. Cells were treated with respective IC_{90} concentrations of CDDP (IC_{90} 2 h/24 h) and **12** (IC_{90} 2 h/24 h) and adherent cells were harvested separately after indicated times (08 h/ 24 h). Further 1411HP cells were treated with respective IC_{90} concentration of CDDP derived from sensitive H12.1 (3 μM). α-Tubulin was used as loading control; FC: floating cells. (B) Activation of caspase -3 after exposure to equitoxic IC_{90} concentrations of CDDP and **12** investigated by substrate cleavage assay. Caspase -3 activity was evaluated by OD ratio of treated/untreated adherent cells. Values represent means of three independent experiments. (C) Western blot analyses of caspase -3 cleavage in presence of caspase-specific inhibitor. H12.1 and 1411HP were treated with Z-VAD-Fmk [60 μM] 2 h prior exposure to equitoxic IC_{90} concentrations of CDDP or **12** (IC_{90} 24 h) and adherent and floating cells were harvested after 24 h and 48 h. α-Tubulin was carried along as loading control. The decreased α-Tubulin line visible in **12**-exposed H12.1 and 1411HP cells can be assigned to progressed apoptosis and cellular degradation. (D) Apoptotic cell death in floating H12.1 and 1411HP cells exposed to **12** and caspase-specific inhibitor was confirmed by DNA laddering. After pretreatment with Z-VAD-Fmk [60 μM, 2 h] **12** (IC_{90} 2 h/24 h) was added for 24 h. Lane 1 H12.1 **12** 2.5 μM + Z-VAD-Fmk 60 μM, lane 2 1411HP **12** 2.5 μM + Z-VAD-Fmk 60 μM.

release in both cell models and a significant formation of ROS in resistant 1411HP cells.

Discussion

The development of alternate platinum compounds possessing the ability to circumvent CDDP resistance is anymore a key ingredient of platinum research. This study was undertaken to evaluate the cytotoxic potential of new CDDP derivatives **1**−**12** in human TGCT cell lines. We found a clear structure−effect relationship in the way that efficacy of substances correlated with their THP-alkyl spacer length and differed dependent on the link of spacer to CDDP. **12** showed the strongest cytotoxic activity and completely overcame intrinsic CDDP-resistance of both 1411HP and 1777NRpmet cell lines. At this, efficacy of **12** is essentially linked to the platinum moiety. A potential mechanism of the promising potency of **12** could be the high cellular accumulation, suggesting a strong relationship between drug cytotoxicity and uptake. Indeed, as compared to CDDP and structural comparable THP compounds with shorter alkyl chain length, **12** treatment caused much higher cellular platinum accumulation. Moreover, the high apoptotic threshold of CDDP-resistant 1411HP cells was overcome by selective stronger

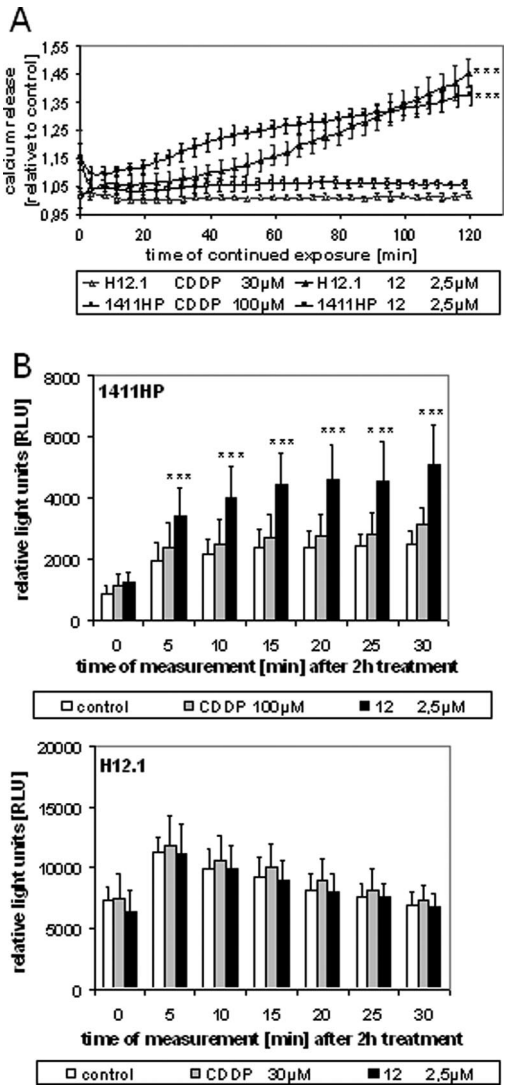

Figure 5. Investigations of alternate putative mediators in apoptosis initiated by CDDP and **12** in H12.1 and 1411HP cells. Values represent means ± SD of three independent experiments. (A) Cytosolic calcium release after continued exposure to equitoxic IC_{90} concentrations of CDDP and **12** for 2 h. Values represent means relative to control (***: significant to CDDP, $p < 0{,}001$). (B) Analysis of superoxide anion radical ($O_2^{-\bullet}$) formation after treatment with equitoxic IC_{90} concentrations of CDDP and **12** for 2 h using lucigenin assay (***: significant to control, $p < 0{,}001$).

accumulation of **12** by assuming increased permeability or transport across their membranes. The exact reason remains unclear, however, it is possibly related to the lipophilic character of the alkyl spacer, facilitating a more easily penetration of cellular membrane. Our results are in agreement with published data, which likewise showed a correlation between efficacy and uptake of lipophilic platinum drugs into different tumor models.[30]

It is commonly accepted that CDDP exerts its cytotoxic effects by covalent binding to genomic DNA.[31] Binding to mitochondrial DNA is discussed controversial but in general will be ascribed a subordinate importance for its activity. As no direct correlation of drug accumulation respectively DNA platination and CDDP sensitivity is given, it is suggested that CDDP-induced toxicity is not entirely DNA-dependent and protein damage may be involved as well.[10,32] Despite its high drug uptake, DNA platination by **12** is much less than by CDDP. This low DNA reactivity may explained by the molecule size and steric hindrance of linking the platinum to DNA. Our results revealed for the first time that a platinum substance in defiance of its high cytotoxic potency evinces only weak DNA interactions. The altered and decreased DNA binding mode of **12** may be responsible for the different cellular responses and damage in the examined TGCT panel in contrast to CDDP.

The anticancer activity of CDDP is mediated by apoptotic cell death after cellular damage passes a critical threshold level. Both the "intrinsic" mitochondrial-interceded pathway and the "extrinsic" death receptor-induced pathway culminate in initiation of caspase cascade and in an irreversible cellular commitment to and execution of apoptosis. Cleavage and inactivation of PARP by caspase -3 is a defined characteristic of CDDP-induced apoptosis in different TGCT cell lines.[33] As shown in our studies, CDDP-triggered apoptosis was proven by creation of floating H12.1 and 1411HP cells, which display typical DNA fragmentation. Also, caspase -3 was cleaved and activated after 24 h exposure accompanied by cleavage of PARP. Equally, **12** induced fragmentation of DNA in floating H12.1 and 1411HP cells and seemed to activate cellular apoptotic processes in a similar degree. Cleavages of caspase -3 and PARP as well as release of cytochrome c into cytosol (data not shown) occurred, but **12** engendered accelerated caspase -3 and PARP cleavages and quicker cytochrome c release than CDDP. The pattern of quick caspase -3 activation ("caspase storm") initiated by **12** is consistent with previously made observations in H12.1 and 1411HP cells for caspase -2, -8, and -9 (data not shown).

It is generally recognized that apoptosis triggered by CDDP correlates with upregulation of p53. p53-mediated arrest at G_1/S-checkpoint permits DNA repair before replication, whereas an arrest at G_2/M-checkpoint allows repair before chromosome separation.[16] Results to date prove that CDDP-damaged DNA causes a transient S-phase arrest followed by G_2/M arrest. In the event of irreparable DNA damage, apoptosis is induced.[11,15] Correlating with existing data CDDP caused p53 accumulation after 8 h and 24 h drug exposure in H12.1 and 1411HP cells as well as an S-phase arrest in H12.1 and slight accumulation in 1411HP after 24 h treatment. In contrast, nearly no modulation of p53 was found in both cell lines after 8 h and 24 h exposure to **12**, which was paralleled by lack of cell cycle arrest and the observed much lower DNA platination rate. Consequently, **12** seems to activate presumably a p53- and cell cycle-independent pathway of apoptosis in contrast to the nucleus-dependent pathway triggered by CDDP.

Besides the classical caspase-dependent apoptosis, also caspase-independent programmed cell death may occur, maintaining key characteristics of apoptosis. The specific mechanisms have not yet been completely identified, but caspase activation seems to participate only in formation of apoptotic morphology.[34,35] We could confirm that CDDP-initiated apoptosis in TGCT proceeds by the caspase-mediated pathway because pretreatment with Z-VAD-Fmk blocked formation of floating cells after CDDP treatment in both H12.1 and 1411HP for 24 h and 48 h. Notably, **12** bypassed the caspase-dependent mechanism evinced by occurrence of floating cells showing typical DNA fragmentation despite of treatment with Z-VAD-Fmk after 24 h and 48 h. Cellular responses to **12** indicate that caspases are nonessential effectors of its apoptotic program but facilitate its execution. They seem to be activated as downstream events and more as a sign rather than mechanistic feature of **12**-triggered cell death. Thus, **12** overcame the death barrier in TGCT cells by offence of an extranuclear, nonclassical apoptotic pathway manifesting in a widely DNA-, p53-, and cell cycle-independent cell damage.

At this, a possibly stress-induced damage of organelles, like endoplasmatic reticulum (ER) or mitochondria, could be discussed.

Mitochondria and ER integrities are central for cell viability having charge of ATP and protein synthesis and regulating calcium, ROS, and pH homeostasis. On the other hand, they play a pivotal initiating role as stress sensors and executioners in response to death triggers. Perturbations of calcium status lead to ER stress response, resulting in calcium release into cytosol and activation of calcium-dependent enzymes.[36,37] Recent studies showed a CDDP-triggered ER stress in enucleated human colon cancer and melanoma cells causing a calcium-dependent activation of calpain.[38] Increased cytosolic calcium and calpain activation may evoke stimulation of ER membrane-associated caspase -12, which may directly process caspase -9 and -3.[36,39] Further, mitochondrial serine protease Omi/High temperature requirement A2 (Omi/HtrA2) is released to cytoplasm during ER stress, where it influences the progression of caspase-dependent and -independent apoptosis.[40] Mitochondria act as a safety device against cytosolic calcium overload, which in turn induces permeability transition pore (PTP) opening after overcoming a critical threshold.[41] Besides, PTP opening is mediated by oxidative stress or direct interactions with cytotoxic agents, leading to mitochondrial leakage of apoptogenic factors and initiation of caspase-dependent and -independent apoptosis. Calcium and ROS are potent inducers of PTP opening, and excessive mitochondrial dysfunction is associated with an increase in cytosolic calcium and formation of ROS.[42,43] ROS damage nucleic acids and proteins and cause lipid peroxidation of plasma membrane. It was demonstrated that also CDDP-mediated apoptosis can be accompanied by increase in ROS generation.[44] An acute stress-elicited apoptosis initiated by ROS formation could be observed in enucleated colon carcinoma and melanoma cells treated with CDDP.[45] Our analyses revealed significantly increased level of cytosolic calcium in both H12.1 and 1411HP cells after exposure to **12** in contrast to CDDP, confirming the suspicion of a stress-induced apoptotic signal transduction. Further, treatment of 1411HP with **12** provoked significant ROS generation compared with CDDP. Interestingly, in H12.1 cells exposed to **12** as well as in both H12.1 and 1411HP treated with CDDP, no significant stimulation of ROS formation was observed. Participation of ROS in the apoptotic response to **12** in 1411HP cells could also be confirmed by superoxide scavenger *N*-acetylcysteine, leading to decreased susceptibility to **12** (data not shown).

Taken together, **12** is able to completely overcome CDDP resistance of human TGCT cell line 1411HP correlating with a strengthened efficacy and multiple higher uptake as compared to CDDP. Considering the molecular features induced by **12** bypassing widely DNA damage as well as p53-, cell cycle-, and caspase-dependent processes and triggering stress-induced mitochondrial and ER-pathways, assuming that **12** and CDDP act by different apoptotic mechanisms. Calcium and ROS seem to be considered mediators in an early phase of **12**-provoked apoptosis. First preclinical in vivo-studies using iv applied **12**-micelles inclusion compounds in nude mice evinced minor side effects compared to CDDP and warrants further in vivo and in vitro tests of this promising platinum compound.

Experimental Section

Platinum Compounds. 1−12 were synthesized by Paschke et al.[27–29] CDDP was obtained from Sigma-Aldrich Chemical Co. (Taufkirchen, Germany). Drugs were dissolved in *N*,*N*-dimethylformamide (DMF, Sigma-Aldrich) to a final concentration of 20 mM and stored at 2−8 °C.

TGCT Cell Lines and Culture Conditions. The human TGCT cell lines H12.1, H12.5, 833K, 2102EP, 577MF, 1777NRpmet, and 1411HP were included in this study. H12.1 and H12.5 were established from an orchiectomy specimen of a 19 year-old previously untreated patient.[46] The TGCT cell lines 833K, 2102EP, 577MF, 1777NRpmet, and 1411HP were kindly provided by Prof. Peter W. Andrews (University of Sheffield, UK).[47,48] Cultures maintained a monolayer in RPMI 1640 (PAA Laboratories, Pasching, Germany) supplemented with 10% heat-inactivated fetal bovine serum (Biochrom AG, Berlin, Germany) and penicillin/streptomycin (PAA Laboratories) at 37 °C in a humidified atmosphere of 5% CO_2/95% air.

Cytotoxicity Assay. The cytotoxic activities of the platinum compounds were evaluated using the sulforhodamine-B (SRB) (Sigma-Aldrich) microculture colorimetric assay.[49] Briefly, exponentially growing cells were seeded into 96-well plates on day 0 at the appropriate cell densities to prevent confluence of the cells during the period of the experiment. After 24 h, cells were treated with serial dilutions of CDDP or the THP platinum compounds (0−100 μM) for 2 h or 96 h and in the case of 2 h treatment washed thoroughly with phosphate-buffered saline (PBS) and further grown in drug-free media for additional 94 h. The final concentration of DMF solvent in the culture medium never exceeded 0.5%, which was nontoxic to the cells. Percentages of surviving cells relative to untreated controls were determined 96 h after beginning of drug exposure. After processing of the 96-well plates according to published SRB assay protocol, absorbance was measured at 570 nm using a 96-well plate reader (SpectraFluor Plus Tecan, Crailsheim, Germany). The IC_{50} and IC_{90} values defined as the drug concentrations that inhibit cell growth by 50% and 90% were estimated graphically from semilogarithmic concentration−response plots.

Platinum Drug Accumulation and DNA Platination Studies. For platinum uptake studies, cell lines H12.1 and 1411HP were seeded into 60 cm^2 tissue culture dishes, and after 24 h, exponentially growing cells were exposed to equimolar (30 μM) or equitoxic IC_{90} concentrations of CDDP, **9**, **10**, and **12** for 2 h. Following treatment with drugs, adherent cells were immediately washed with PBS to remove free platinum, harvested by trypsinization, and dried. Platinum concentrations were measured by flameless atomic absorption spectroscopy (AAS) using an AAS-5 EA including the semiautomatic solid sampling dispensing system SSA 51 (Analytic Jena AG, Germany) and expressed as platinum content [ppm] in lyophilized cells (original weight always 20−300 μg). For determination of platinum bound to DNA H12.1 and 1411HP were exposed to equimolar concentrations (30 μM) of CDDP or **12** for 6 h. Floating cells were discarded and adherent cells were harvested, washed twice with PBS, and genomic DNA was extracted according to standard procedures using the Blood & Cell Culture DNA Kit (Qiagen Chemical Company, Hilden, Germany). DNA-bound platinum amounts were determined by AAS and expressed as platinum content [ppm] in lyophilized genomic DNA (original weight always 20−300 μg).

DNA Fragmentation Assay. Determination of apoptotic cell death was performed by DNA gel electrophoresis. Briefly, H12.1 and 1411HP were treated with respective IC_{90} concentrations of CDDP or **12** for 24 h. Floating cells induced by drug exposure were collected, washed twice with PBS, and lysed in lyses-buffer (100 mM Tris-HCl pH 8.0, 20 mM EDTA, 0.8% SDS) (all from Sigma-Aldrich). After treatment with RNase A at 37 °C for 2 h and proteinase K (both Roche Diagnostics Chemical Company, Mannheim, Germany) at 50 °C overnight, DNA laddering was visualized by running probes on a 2% agarose gel followed by ethidium bromide (Sigma-Aldrich) staining.

Western Blot Analysis. After 8 h and 24 h drug exposure to equitoxic IC_{90} concentrations of CDDP or **12** using a 2 h/96 h treatment schedule, adherent cells were harvested by trypsinization and Western blot analyses were performed. Protein concentrations were determined using the Bio-Rad protein assay (Bio-Rad Laboratories, Munich, Germany). 30 μg of total cell proteins were electrophoresed on a 15% sodium dodecyl sulfate (SDS)-polyacrylamide gel and blotted on nitrocellulose (Whatman Chemical

Company, Dassel, Germany). Equal loading was checked by red Ponceau S (Sigma-Aldrich) staining. Membranes were pre-blocked in 5% nonfat dry milk in PBST (containing 0.1% Tween 20 (Sigma-Aldrich) in PBS) for 1 h and subsequently incubated for a further 2 h in 5% nonfat dry milk in PBST supplemented with specific antibodies against caspase -3 mouse monoclonal IgG (0.5 μg/mL, MBL/Biozol Diagnostica, Eching, Germany), p53 (Do-1) mouse monoclonal IgG (0,5 μg/mL, Santa Cruz Biotechnology Inc., Santa Cruz, CA) and PARP mouse monoclonal IgG (0.5 μg/mL, BD Biosciences PharMingen, Heidelberg, Germany). Mouse monoclonal IgG anti-Tubulin-α Ab-2 antibody (0.5 μg/mL, Dianova Chemical Company, Hamburg, Germany) served to confirm the presence of equal amounts of protein within each lane. After washing and incubation with horseradish peroxidase-conjugated goat antimouse IgG (1:5000, Santa Cruz Biotechnology Inc.) immunological complexes were visualized using chemiluminescence (ECL) detection system (Amersham Pharmacia Biotech, Little Chalfont, UK). Blots were repeated at least two times.

Cell Cycle Analysis. Cell cycle perturbations induced by CDDP or **12** were investigated in exponentially growing cells of H12.1 and 1411HP. After treatment with equitoxic IC_{90} drug concentrations for 8, 24, 48, and 72 h cells were harvested by trypsinization at indicated time points. Both floating and adherent cells were combined, washed with cold PBS, and fixed with ethanol 70% (Roth Chemical Company, Karlsruhe, Germany). After storage at 4 °C and centrifugation, cells were washed with staining buffer (PBS, 2% fetal bovine serum, 0.01% NaN_3 (Sigma-Aldrich)), centrifuged again, and incubated with RNase A for 1 h at 37 °C. After it, cells were stained with propidium iodide (Sigma-Aldrich) for 30 min and fluorescence intensity was determined by a Facscalibur (Becton Dickinson, Heidelberg, Germany). Each analysis was done using about 1×10^4 events.

Caspase -3 Enzyme Activity Assay. Activity of caspase -3 was measured using the caspase substrate cleavage assay. After exposure to equitoxic IC_{90} concentrations of CDDP or **12**, cells were sampled each hour for cleavage of caspase -3 over an assay period of maximal 34 h. To summarize, adherent cells were washed with cold PBS, collected with a cell scraper, and suspended in cell lyses buffer (50 mM Hepes pH 7.4, 1% Triton X100, all from Sigma-Aldrich). After incubation for 10 min on ice and centrifugation, protein concentrations of the supernatants were measured according to method of Bradford (Bio-Rad Laboratories). Samples (50 μg protein extract respectively) were incubated on a microplate at 37 °C overnight in reaction buffer (50 mM Hepes pH 7.4, 0.1% CHAPS, 5 mM EGTA, 5% glycerol) containing 10 mM DTT (all from Sigma-Aldrich) and a specific substrate of caspase -3 (Ac-DEVD-pNA, Axxora, Lörrach, Germany). Extinction of released *p*-nitroaniline was measured at 405 nm (SpectraFluor Plus Tecan) and activity of caspase -3 was evaluated by OD ratio of treated/untreated samples.

Calcium Release Studies. To investigate the intracellular calcium levels of cell lines H12.1 and 1411HP after drug treatment, cells were seeded with nearly confluence into 96-well plates. After 24 h, cells were exposed to equitoxic IC_{90} concentrations of CDDP or **12** and released intracytosolic calcium was measured fluorimetrically for 2 h using the PBX calcium assay kit (BD Biosciences PharMingen). Increase of cytosolic calcium level was ascertained by ratio of treated/untreated samples.

Lucigenin Assay. Analysis of superoxide anion radical ($O_2^{-\cdot}$) production was performed by the lucigenin method. Briefly, H12.1 and 1411HP were seeded into 6-well plates, and after 48 h, confluent grown cells were treated with equitoxic IC_{90} concentrations of CDDP or **12** for 2 h. Following exposure, cells were washed with cold PBS, incubated with trypsin for 1 min and suspended in PBS. Measurement of chemiluminescence was started by adding 50 μM lucigenin (bis-*N*-methylacridiniumnitrate) and 100 μM NADPH (both Sigma-Aldrich) using a luminometer Lumat LB 9507 (Berthold Technologies, Bad Wildbad, Germany). Photon emission was counted every 5 min for up to 30 min.

Data Analysis. Results were calculated as means $\pm$ standard deviation (SD) of three independent experiments. To compare several treatment groups, data were tested for significance accepting a significance level of at least $p < 0.05$ using one-way analysis of variance (ANOVA) followed by multiple comparison test of Bonferroni.

Acknowledgment. This work was supported by a grant from the "Kultusministerium Sachsen-Anhalt" PA3573B/0604T. We thank U. Hinkelmann (Department of Pharmacology and Toxicology, Institute of Pharmacy, Martin-Luther-University of Halle-Wittenberg) for technical assistance with quantification of ROS.

References

(1) Voigt, W.; Dietrich, A.; Schmoll, H.-J. Overview of development status and clinical action. Cisplatin and its analogues. *Pharm. Unserer Zeit* **2006**, *35* (2), 134–143.
(2) Lebwohl, D.; Canetta, R. Clinical development of platinum complexes in cancer therapy: an historical perspective and an update. *Eur. J. Cancer* **1998**, *34,* (10), 1522–1534.
(3) Einhorn, L. H. Curing metastatic testicular cancer. *Proc. Natl. Acad. Sci. U.S.A.* **2002**, *99* (7), 4592–4595.
(4) Masters, J. R.; Köberle, B. Curing metastatic cancer: lessons from testicular germ-cell tumours. *Nat. Rev. Cancer* **2003**, *3* (7), 517–525.
(5) Spierings, D. C.; de Vries, E. G.; Vellenga, E.; de Jong, S. The attractive achilles heel of germ cell tumours: an inherent sensitivity to apoptosis-inducing stimuli. *J. Pathol.* **2003**, *200* (2), 137–148.
(6) Kollmannsberger, C.; Nichols, C.; Bokemeyer, C. Recent advances in management of patients with platinum-refractory testicular germ cell tumors. *Cancer* **2006**, *106* (6), 1217–1226.
(7) Safaei, R.; Howell, S. B. Copper transporters regulate the cellular pharmacology and sensitivity to Pt drugs. *Crit. Rev. Oncol. Hematol.* **2005**, *53* (1), 13–23.
(8) Ho, Y. P.; Au-Yeung, S. C.; To, K. K. Platinum-based anticancer agents: innovative design strategies and biological perspectives. *Med. Res. Rev.* **2003**, *23* (5), 633–655.
(9) Bose, R. N. Biomolecular targets for platinum antitumour drugs. *Mini Rev. Med. Chem.* **2002**, *2* (2), 103–111.
(10) Fuertes, M. A.; Alonso, C.; Perez, J. M. Biochemical modulation of cisplatin mechanisms of action: enhancement of antitumor activity and circumvention of drug resistance. *Chem. Rev.* **2003**, *103* (3), 645–662.
(11) Eastman, A. Activation of programmed cell death by anticancer agents: cisplatin as a model system. *Cancer Cells* **1990**, *2* (8−9), 275–280.
(12) Fan, T. J.; Han, L. H.; Cong, R. S.; Liang, J. Caspase family proteases and apoptosis. *Acta Biochim. Biophys. Sin. (Shanghai)* **2005**, *37* (11), 719–727.
(13) Boatright, K. M.; Salvesen, G. S. Mechanisms of caspase activation. *Curr. Opin. Cell Biol.* **2003**, *15* (6), 725–731.
(14) Budihardjo, I.; Oliver, H.; Lutter, M.; Luo, X.; Wang, X. Biochemical pathways of caspase activation during apoptosis. *Annu. Rev. Cell Dev. Biol.* **1999**, *15*, 269–290.
(15) Siddik, Z. H. Cisplatin: mode of cytotoxic action and molecular basis of resistance. *Oncogene* **2003**, *22* (47), 7265–7279.
(16) Schafer, K. A. The cell cycle: a review. *Vet. Pathol.* **1998**, *35* (6), 461–478.
(17) Gonzales, V. M.; Fuertes, M. A.; Alonso, C.; Perez, J. M. Is cisplatin-induced cell death always produced by apoptosis? *Mol. Pharmacol.* **2001**, *59* (4), 657–663.
(18) Perez, R. P. Cellular and molecular determinants of cisplatin resistance. *Eur. J. Cancer* **1998**, *34* (10), 1535–1542.
(19) Jakupec, M. A.; Galanski, M.; Keppler, B. K. Tumour-inhibiting platinum complexes: state of the art and future perspectives. *Rev. Physiol. Biochem. Pharmacol.* **2003**, *146*, 1–54.
(20) Wong, E.; Giandomenico, C. M. Current status of platinum-based antitumor drugs. *Chem. Rev.* **1999**, *99* (9), 2451–2466.
(21) Servidei, T.; Ferlini, C.; Riccardi, A.; Meco, D.; Scambia, G.; Segni, G.; Manzotti, C.; Riccardi, R. The novel trinuclear platinum complexes BBR3464 induces a cellular response different from cisplatin. *Eur. J. Cancer* **2001**, *37* (7), 930–938.
(22) Kasparkova, J.; Zehnulova, J.; Farrell, N.; Brabec, V. DNA interstrand cross-links of the novel antitumor trinuclear platinum complex BBR3464. Conformation, recognition by high mobility group domain proteins, and nucleotide excision repair. *J. Biol. Chem.* **2002**, *277* (50), 48076–48086.
(23) Criado, J. J.; Herrera, M. C.; Palomero, M. F.; Medarde, M.; Rodriguez, E.; Marin, J. J. Synthesis and characterization of a new bile acid and platinum(II) complex with cytostatic activity. *J. Lipid Res.* **1997**, *38* (5), 1022–1032.

(24) Marin, J. J.; Macias, R. I.; Criado, J. J.; Bueno, A.; Monte, M. J.; Serrano, M. A. DNA interaction and cytostatic activity of the new liver organotropic complex of cisplatin with glycocholic acid: Bamet-R2. *Int. J. Cancer* **1998**, *78* (3), 346–352.
(25) Dominguez, M. F.; Macias, R. I.; Izco-Basurko, I.; de La Fuente, A.; Pascual, M. J.; Criado, J. M.; Monte, M. J.; Yajeya, J.; Marin, J. J. Low in vivo toxicity of a novel cisplatin-ursodeoxycholic derivative (Bamet-UD2) with enhanced cytostatic activity versus liver tumors. *J. Pharmacol. Exp. Ther.* **2001**, *297* (3), 1106–1112.
(26) Paschke, R.; Paetz, C.; Mueller, T.; Schmoll, H. J.; Mueller, H.; Sorkau, E.; Sinn, E. Biomolecules linked to transition metal complexes: new chances for chemotherapy. *Curr. Med. Chem.* **2003**, *10* (19), 2033–2044.
(27) Paschke, R.; Kalbitz, J.; Paetz, C.; Luckner, M.; Mueller, T.; Schmoll, H.-J.; Mueller, H.; Sorkau, E.; Sinn, E. Cholic acid−carboplatin compounds (CarboChAPt) as models for specific drug delivery: synthesis of novel carboplatin analogous derivatives and comparison of the cytotoxic properties with corresponding cisplatin compounds. *J. Inorg. Biochem.* **2003**, *94* (4), 335–342.
(28) Paschke, R.; Kalbitz, J.; Paetz, C. Novel spacer linked bile acid−cisplatin compounds as a model for specific drug delivery, synthesis and characterization. *Inorg. Chim. Acta* **2000**, *304*, 241–249.
(29) Paschke, R.; Voigt, W.; Mueller, T.; Kalbitz, J.; Maeder, K.; Dietrich, A. Platinum(II) compounds from 2-substituted propane-1,3-diamines for use as antitumor chemotherapeutic drugs. German Patent DE 102005047308 A1 20070405 AN, 385077, 2007.
(30) Ang, W. H.; Pilet, S.; Scopelliti, R.; Bussy, F.; Jiullerat-Jeanneret, L.; Dyson, P. J. Synthesis and characterization of platinum(IV) anticancer drugs with functionalized aromatic carboxylate ligands: influence of the ligands on drug efficacies and uptake. *J. Med. Chem.* **2005**, *48* (25), 8060–8069.
(31) Jamieson, E. R.; Lippard, S. J. Structure, recognition, and processing of cisplatin-DNA adducts. *Chem. Rev.* **1999**, *99* (9), 2467–2498.
(32) Yang, Z.; Schumaker, L. M.; Egorin, M. J.; Zuhowski, E. G.; Guo, Z.; Cullen, K. J. Cisplatin preferentially binds mitochondrial DNA and voltage.dependent anion channel protein in the mitochondrial membrane of head and neck squamous cell carcinoma: possible role in apoptosis. *Clin. Cancer Res.* **2006**, *12* (19), 5817–5825.
(33) Burger, H.; Nooter, K.; Boersma, A. W.; Kortland, C. J.; Stoter, G. Lack of correlation between cisplatin-induced apoptosis, p53 status and expression of Bcl-2 family proteins in testicular germ cell tumour cell lines. *Int. J. Cancer* **1997**, *73* (4), 592–599.
(34) Kroemer, G.; Martin, S. J. Caspase-independent cell death. *Nat. Med.* **2005**, *11* (7), 725–730.
(35) Donovan, M.; Cotter, T. G. Control of mitochondrial integrity by Bcl-2 family members and caspase-independent cell death. *Biochim. Biophys. Acta* **2004**, *1644* (2−3), 133–147.
(36) Rao, R. V.; Ellerby, H. M.; Bredesen, D. E. Coupling endoplasmic reticulum stress to the cell death program. *Cell Death Differ.* **2004**, *11* (4), 372–380.
(37) Orrenius, S.; Zhivotovsky, B.; Nicotera, P. Regulation of cell death: the calcium−apoptosis link. *Nat. Rev. Mol. Cell Biol.* **2003**, *4* (7), 552–565.
(38) Mandic, A.; Hansson, J.; Linder, S.; Shoshan, M. C. Cisplatin induces endoplasmic reticulum stress and nucleus-independent apoptotic signaling. *J. Biol. Chem.* **2003**, *278* (11), 9100–9106.
(39) Morishima, N.; Nakanishi, K.; Takenouchi, H.; Shibata, T.; Yasuhiko, Y. An endoplasmic reticulum stress-specific caspase cascade in apoptosis. *J. Biol. Chem.* **2002**, *277* (37), 34287–34294.
(40) Cilenti, L.; Kyriazis, G. A.; Soundarapandian, M. M.; Stratico, V.; Yerkes, A.; Park, K. M.; Sheridan, A. M.; Alnemri, E. S.; Bonventre, J. V.; Zervos, A. S. Omi/HtrA2 protease mediates cisplatin-induced cell death in renal cells. *Am. J. Physiol. Renal. Physiol.* **2005**, *288* (2), F371−F379.
(41) Smaili, S. S.; Hsu, Y.-T.; Youle, R. J.; Russell, J. T. Mitochondria in Ca^{2+} signaling and apoptosis. *J. Bioenerg. Biomembr.* **2000**, *32* (1), 35–46.
(42) Chakraborti, T.; Das, S.; Mondal, M.; Roychoudhury, S.; Chakraborti, S. Oxidant, mitochondria and calcium: an overview. *Cell. Signal.* **1999**, *11* (2), 77–85.
(43) Raha, S.; Robinson, B. H. Mitochondria, oxygen free radicals, and apoptosis. *Am. J. Med. Genet.* **2001**, *106* (1), 62–70.
(44) Salganik, R. I. The benefits and hazards of antioxidants: controlling apoptosis and other protective mechanisms in cancer patients and the human population. *J. Am. Coll. Nutr.* **2001**, *20* (5), 464S–472S.
(45) Berndtsson, M.; Hägg, M.; Panaretakis, T.; Havelka, A. M.; Shoshan, M. C.; Linder, S. Acute apoptosis by cisplatin requires induction of reactive oxygen species but is not associated with damage to nuclear DNA. *Int. J. Cancer* **2006**, *120* (1), 175–180.
(46) Casper, J.; Schmoll, H.-J.; Schnaidt, U.; Fonatsch, C. Cell lines of human germinal cancer. *Int. J. Androl.* **1987**, *10* (1), 105–113.
(47) Wang, N.; Trend, B.; Bronson, D. L.; Fraley, E. E. Nonrandom abnormalities in chromosome 1 in human testicular cancers. *Cancer Res.* **1980**, *40* (3), 796–802.
(48) Vogelzang, N. J.; Bronson, D.; Savino, D.; Vessella, R. L.; Fraley, E. F. A human embryonal yolk sac carcinoma model system in athymic mice. *Cancer* **1985**, *55* (11), 2584–2593.
(49) Skehan, P.; Storeng, R.; Scudiero, D.; Monks, A.; McMahon, J.; Vistica, D.; Warren, J. T.; Bokesch, H.; Kenney, S.; Boyd, M. R. New colorimetric cytotoxicity assay for anticancer-drug screening. *J. Natl. Cancer Inst.* **1990**, *82* (13), 1107–1112.

JM800334Z